"BABEŞ-BOLYAI" UNIVERSITY
Faculty of Chemistry and Chemical Engineering

MACROCYCLIC LIGANDS (PERAZA CROWN) AND THEIRS NEW COMPLEXES WITH TRANSITIONAL METALS

PhD. THESIS

Mihaela Cecilia VLASSA

Scientific advisor:
Prof. Dr. Cristian SILVESTRU

Cluj-Napoca
2011

"BABEŞ-BOLYAI" UNIVERSITY
Faculty of Chemistry and Chemical Engineering

MACROCYCLIC LIGANDS (PERAZA CROWN ETHERS) AND THEIRS NEW COMPLEXES WITH TRANSITIONAL METALS

PhD. Thesis

ABSTRACT

Mihaela Cecilia VLASSA

Scientific advisor:
Prof. Dr. Cristian SILVESTRU

JURY:

PREZIDENT
Assoc.Prof.dr. CORNELIA MAJDIK Dean of the Faculty of Chemistry and Chemical Engineering, "Babeş-Bolyai" University, Cluj-Napoca

REVIEWERS
Prof. dr. IONEL MANGALAGIU, "Alexandru Ioan Cuza" University Iaşi
Prof. dr. LELIA CIONTEA, Technical University of Cluj-Napoca
Prof. dr. MARIA CURTUI, "Babeş-Bolyai" University Cluj-Napoca

Defence: 27th October 2011

Abreviations

Ac	acetyl
BET	specific surface
BzN_6	3,10-dibenzyl-1,3,5,8,10,12-hexaazacyclotetradecan
bpactde	1,2-bis(1,3,5,8,12-pentaazacyclotetradecane-3-yl)ethane
bpactdb	1,4-bis(1,3,5,8,12-pentaazacyclotetradecane-3-yl)butane
4,4'-bipy	4,4'-bipyridil
ChN_4	6,15-dimethyldocosahydrodibenzo[b,i][1,4,8,11]tetraazacyclo-tetradecane
ciclam	1,4,8,11-tetraazacyclotetradecane
ciclen	1,4,7,10-tetrazacyclododecane
dap	2,3-diaminopropane
DEF	N,N'-diethylformamide
dmdocosan	3,4-dimethyl-2,6,13,17-tetraazatricyclo[14,4,$0^{1.18}$,$0^{7.12}$]docosane
DMF	N,N'-dimethylformamide
DMSO	dimethylsulfoxide
N-rac-dmtacdd	*N-rac*-5,12-dimethyl-1,4,8,11-tetraazacyclotetradeca-4,11-diene
N-dl-dmtacdd	*N-dl*-5,12-dimethyl-1,4,8,11-tetraazacyclotetradeca-4,11-diene
ebsi	ethylenbis(salicilimine)
EtN_6	3,10-diethyl-1,3,5,8,10,12-hexaazacyclotetradecane
hatco	1,3,6,8,11,14-hexaazatricyclooctadecane
H_4atc	adamantane-1,3,5,7-tetracarboxylic acid
H_2(*trans*-1,4-bd)	(*E*)-hex-3-enedioic (*trans*-buten-1,4-dicarboxylic) acid
H_2(1,2-bdc)	benzene-1,2-dicarboxylic acid
H_2(1,3-bdc)	izophtalic acid (benzene-1,3-dicarboxylic acid)
H_2(1,3-bdc-5-OH)	5-hydroxy-izophtalic acid (benzene-5-hydroxy-1,3-dicarboxylic acid)
H_2(1,4-bdc)	benzene-1,4-dicarboxylic acid (terephtalic acid)
H_2bpdc	(1,1'-biphenyl)-4,4'-dicarboxylic acid
H_2bpdes	2,2'-[(1,1'- biphenyl)-4,4'-diyl]diethynsulfonic acid
H_4(2,2‘,6,6‘-bptc)	1,1‘-biphenyl-2,2‘,6,6‘-tetracarboxylic acid
H_4(3,3‘,5,5‘-bptc)	1,1‘-biphenyl-3,3‘,5,5‘-tetracarboxylic acid
H_2bpydc	(2,2'-bipyridyl)-5,5'-dicarboxylic acid
H_2bqdc	(2,2'-biquinoline)-4,4'-dicarboxylic acid
H_3(1,3,5-btb)	5'-(4-carboxyphenyl)-[1,1':3',1''-terphenyl]-4,4''-dicarboxylic acid
H_3(1,3,5-btc)	benzene-1,3,5-tricarboxylic acid
H_4(1,2,4,5-btetc)	benzene-1,2,4,5-tetracarboxylic acid
H_3(1,3,5-ctc)	*cis,cis*-(1*s*,3*s*,5*s*)-cyclohexane-1,3,5-tricarboxylic acid

H_2fum	fumaric acid
H_2hpdc	4,5,9,10-tetrahydropyrene-2,7-dicarboxylic acid
Hinct	izonicotinic acid
H_2male	maleic acid
H_2(2,6-ndc)	naftaline-2,6-dicarboxylic acid
H_2(1,5-nds)	naftaline-1,5-disulfonic acid
H_3ntb	4,4',4''- nitrilotribenzoic acid
H_2ox	oxalic acid
H_2(2,5-pdc)	2,5-pyridinedicarboxylic acid
H_2(2,6-pdc)	2,6- pyridinedicarboxylic acid
H_4tcm	4,4'-[(2,2-bis{(4-carboxyphenoxi)methyl}propane-1,3-diyl)bis(oxi)] dibenzoic acid
H_3tcpeb	4,4',4''-(benzene-1,3,5-triyltris(ethyn-2,1-diyl))tribenzoic acid
H_4tmbdc	tetramethylbenzene-1,4-dicarboxylic acid
H_2ttdc	thieno[3,2-b]tiophene-2,5-dicarboxylic acid
H_2tbdc	*trans*-butene-dicarboxylic acid
IMOF	inverted metal-organic frameworks
mpepactd	13-methyl-6-(1-phenylethyl)-1,4,6,8,11-pentaazacyclotetradecane
mel	2,4,6-tri(1,3,5,8,12-pentaazacyclotetradecan-3-yl)-1,3,5-triazine
MeN_6	3,10-dimethyl-1,3,5,8,10,12-hexaazacyclotetradecane
Me_4N_4	2,5,9,12-tetramethyl-1,4,8,11-tetraazacyclotetradecane
MeCN	acetonitrile
MOF	metal-organic frameworks
MOMN	metal organometallic networks
N,N'-men	N,N'-dimethylethylendiamine
NaK(tart)	sodium and potasiu tartrate
Na_3amrt	trisodium (4*E*)-3-oxo-4-[(4-sulfonato-1-naphthyl) hydrazono] naphthalene-2,7-disulfonate (***amaranth***)
Na_2crmz	disodium 4-hydroxy-2-[(*E*)-(4-sulfonato-1-naphthyl) diazenyl] naphthalene-1-sulfonate (***carmoisine***)
Na_2rcg	disodium 3,3'-([1,1'-biphenyl]-4,4'-diyl)bis(4-aminonaphthalene-1-sulfonate) (***Congo red***)
Na_2ssyw	disodium 6-hydroxy-5-[(4-sulfophenyl)azo]-2-naphthalenesulfononate (***sunset yellow***)
Na_3trt	trisodium(4*E*)-5-oxo-1-(4-sulfonatophenyl)-4-[(4-sulfonatophenyl) hydrazono]-3-pyrazole carboxylate (***tartrazine***)
NEH	5,5,7,13-tetramethyl-13-nitro-1,4,8,11-tetraazacyclotetradecane
NH_4(ox)	amonium oxalate

OHN_6	2,2'-(1,3,5,8,10,12-hexaazacyclotetradecane-3,10-diyl)diethanol
PC	coordination polymer
$PhetN_6$	3,10-diphenethyl-1,3,5,8,10,12-hexaazacyclotetradecane
PhOH	phenol
pm	picometru
$pcltfmSO_3$	polychlorotriphenylmethylsulfonate radical
py	pyridine
PyN_6	3,10-bis(pyridine-4-ylmethyl)-1,3,5,8,10,12-hexaazacyclotetradecane
SBU	secondary building unit
tabpd	6,13-dimethyl-6-nitro-1,4,8,11-tetraazabicyclo[11.1.1]pentadecane
tame	tris(aminomethyl)ethane
tea	triethylamine
tetb	5,5,7,12,12,14-hexamethyl-1,4,8,11-tetraazacyclotetradecane
xyl	1,4-bis((1,3,5,8,12-pentaazacyclotetradecane-3-yl)methyl)benzene

CONTENT

Key words: coordination polymer, aza crown ether, sulfonated aza dye, self-assembling, supramolecular chemistry, crystal structure, hydrogen bonding.

I. INTRODUCTION

The term coordination polymers (CP) is used to denote any extended structure constructed on the basis of metal ions and of organic bridging groups. The first paper in this field appeared in 1959.[1] Structure of another similar material was published after 30 years, namely in 1989.[2] In 1997 were published the first data in connection with the gaze absorption of a such polymer. These kind of materials with adsorption properties were denominated metal organic frameworks (MOF), naming that, initial, were destined to CP-s with porous structures.[4] After 1997, followed a really explosion of publications in connection with synthesis and properties of these materials, till now, being published over 5000 of papers.

The interest for these compounds can be explained by their wide utilisation, having interesting magnetically characteristics,[11-13] electronics[14] and opticals[15] in molecular adsorption processes and separations,[16-18] ionic exchange,[19,20] catalysis,[21,22] sensor[23-25] and optoelectronic[26] technologies, nanotube growths[27] and o series of another applications [28] such as sorption and gaze storages[29,30] including molecular hydrogen.[30-33]

Macrocyclic complexes, that have a square-planar geometry, contain only two *trans* coordination positions, thus acting as linear linkers for ligands. Thus, through utilisation of macrocyclic complexes, it is possible to control extinction of networks direction, simplifying the design and network structure predictions. Moreover, macrocyclic complexes simplify the ligand coordination mode because of the macrocyclic volume.

Taking into consideration, the previously mentioned advantages, due to utilisation of the macrocyclic complexes in the construction of coordination polymers, the aim of this dissertation consists in obtaining of new CP-s where the metallic ion to be complexed by tetradentate azamacrocycles.

As ligands will be used:

- sulfonate azo dyes, the resulted compounds having interesting properties, differentiates comparatively with those of the carboxylate CP-s
- aromatic and aliphatic carboxylates, the last ones being, till now, less used; the structure of its could be influence in positive mode the porosity of obtained materials, according to some theoretical opinions met in the literature[52]

III.1. SULFONATED AZA DYES COORDINATION POLYMERS

Coordination polymers (PC) containing sulfonated azo dyes were prepared using $[M(cyclam)(ClO_4)_2]$ (M = Ni^{2+}, Cu^{2+}, Zn^{2+}) in which metalic cation is complexed with sulfonate groups of the following azo dyes: trisodium(4*E*)-5-oxo-1-(4-sulfonatophenyl)-4-[(4-sulfonatophenyl) hydrazono]-3-pyrazole carboxylate (***tartrazine***; Na_3trt) (**Figure 1a**), disodium 4-hydroxy-2-[(*E*)-(4-

sulfonato-1-naphthyl) diazenyl] naphthalene-1-sulfonate (***carmoisine***; Na_2crmz) (**Figure 1b**), trisodium (4*E*)-3-oxo-4-[(4-sulfonato-1-naphthyl) hydrazono] naphthalene-2,7-disulfonate (***amaranth***; Na_3amrt) (**Figure 1c**), disodium 6-hydroxy-5-[(4-sulfophenyl)azo]-2-naphthalenesulfononate (***sunset yellow***; Na_2ssyw) (**Figure 1d**) and disodium 3,3'-([1,1'-biphenyl]-4,4'-diyl)bis(4-aminonaphthalene-1-sulfonate) ((***Congo red***; Na_2rcg) (**Figure 1e**).

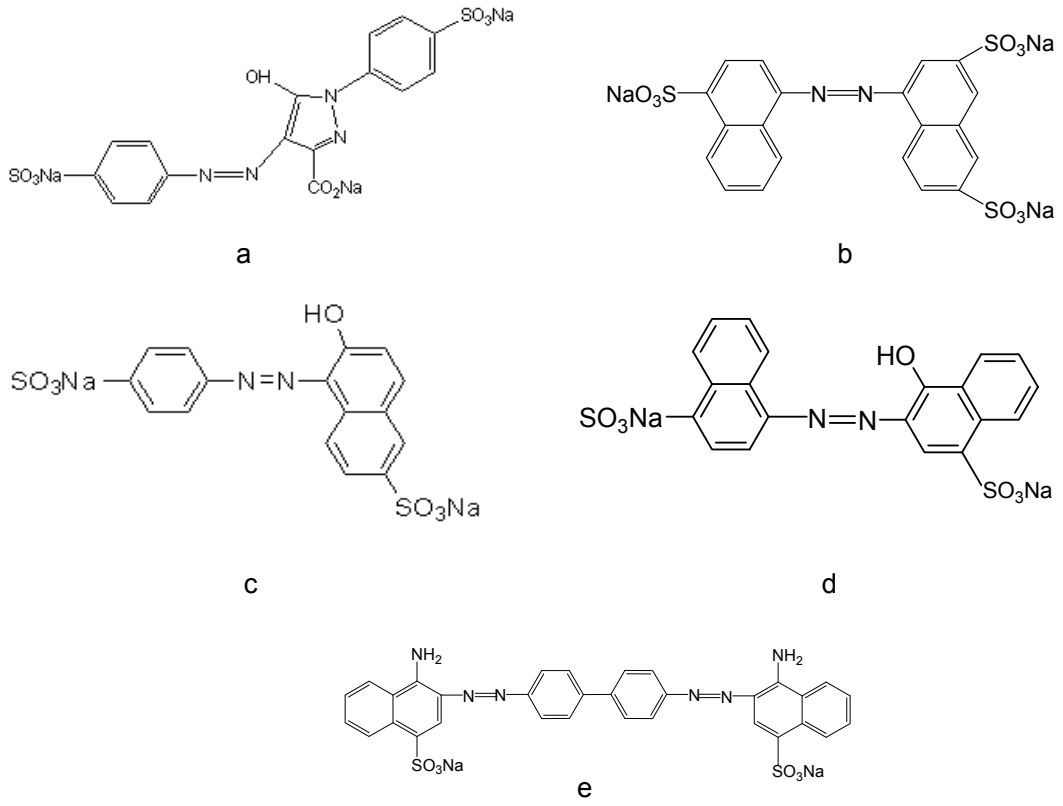

Figure 1. Sulfonated azo dyes used in the synthesis of CP-s.

Obtained polymers have the structure represented by the following formules :

$[\{Cu(cyclam)\}_3(trt)_2\cdot 6H_2O]_n$ (**5**), $[\{Ni(cyclam)\}_3(trt)_2\cdot 43H_2O]_n$ (**6**) and $[\{Zn(cyclam)\}_3(trt)_2\cdot 5H_2O]_n$ (**7**), $[Cu(cyclam)(crmz)\cdot 5H_2O]_n$ (**9**) and $[Ni(cyclam)(crmz)]_n$ (**10**), $[\{Cu(cyclam)\}_3(amrt)_2\cdot 13H_2O]_n$ (**12**), $[\{Ni(cyclam)\}_3(amrt)_2\cdot 4H_2O]_n$ (**13**) and $[\{Zn(cyclam)\}_3(amrt)_2\cdot 14H_2O]_n$ (**14**), $[Ni(cyclam)(ssyw)\cdot 0.5H_2O]_n$ (**16**) $[Cu(cyclam)(rcg)]_n$ (**18**) şi $[Zn(cyclam)(rcg)]_n$ (**19**).

III.1.1. SYNTHESIS OF THE COORDINTION POLYMERS $[\{Cu(ciclam)\}_3(trt)_2\cdot 6H_2O]_n$ (5), $[\{Ni(ciclam)\}_3(trt)_2\cdot 43H_2O]_n$ (6) AND $[\{Zn(ciclam)\}_3(trt)_2\cdot 5H_2O]_n$ (7)

Reaction of $[Cu(cyclam)](ClO_4)_2$ (**2**), $[Ni(cyclam)](ClO_4)_2$ (**3**) or $[Zn(cyclam)](ClO_4)_2$ (**4**), in DMF, with trisodium(4*E*)-5-oxo-1-(4-sulfonatophenyl)-4-[(4-sulfonatophenyl) hydrazono]-3-pyrazole carboxylate (***tartrazine***; Na_3trt) (**1**), in water, produced the following coordination polymers

$[\{Cu(cyclam)\}_3(trt)_2\cdot 6H_2O]_n$ (**5**), $[\{Ni(cyclam)\}_3(trt)_2\cdot 43H_2O]_n$ (**6**) and $[\{Zn(cyclam)\}_3(trt)_2\cdot 5H_2O]_n$ (**7**) (**Scheme 22**).

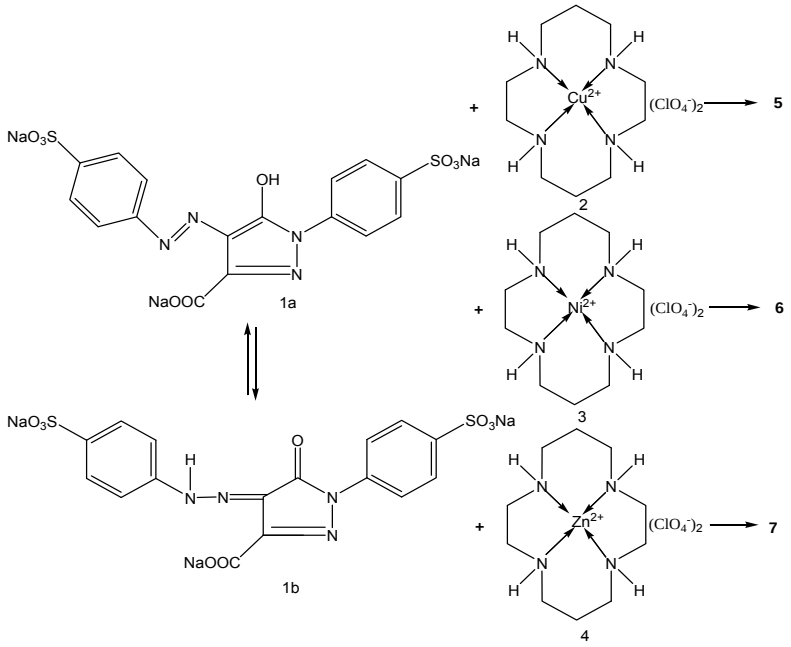

Scheme 22. Preparation reaction scheme of the coordination polymers : $[\{Cu(cyclam)\}_3(trt)_2\cdot 6H_2O]_n$ (**5**), $[\{Ni(cyclam)\}_3(trt)_2\cdot 43H_2O]_n$ (**6**) şi $[\{Zn(cyclam)\}_3(trt)_2\cdot 5H_2O]_n$ (**7**).

III.1.1.1. Characterization of the coordination polymers 5-7 using powder X-ray diffraction

The growth of the single-crystal in the case of compounds **5**-**7** failed, thereby we characterized them, from crystallographic point of view, by means of the powder XRD spectra. As example in **Figure 28** is shown XRPD patterns for $[\{Cu(cyclam)\}_3(trt)_2\cdot 6H_2O]_n$ (**5**). The XRPD patterns of compound **5** are completely different comparatively with those of the starting materials, proving the formation of coordination polymer. Crystal data for coordination polymers **5**-**7**, **9**, **10**, **12**-**14**, obtained from XRPD spectra are shown in **Table 5**.

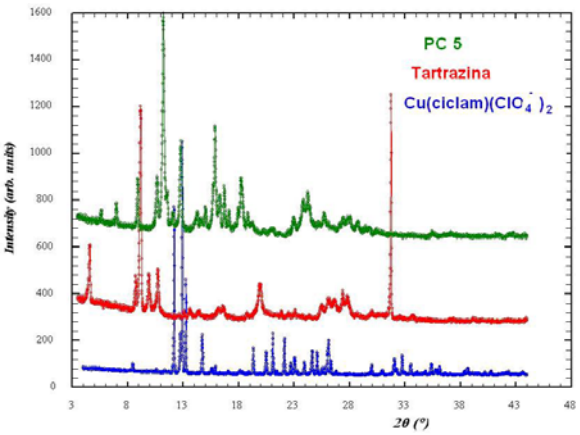

Figure 28. XRPD patterns for $[\{Cu(cyclam)\}_3(trt)_2 \cdot 6H_2O]_n$ (**5**), (up), tartrazine (**1**) (middle) and $[Cu^{2+}(cyclam)](ClO_4)_2$ (**2**) (down).

Table 5. Crystal data for coordination polymers PC **5**-**7**, **9**, **10**, **12**-**14**.

PC	Elementary lattice		Crystal system	Space group	Z	Volume Å^3	$\rho_{calc.}$ g·cm^{-3}	$\rho_{det.}$* g·cm^{-3}
	Å	Grade						
5	a= 15.195(7) b= 19.730(2) c= 24.735(4)	α=β=γ=90	orthorhombic	$Pna2_1$	4	7416	1.520	1.485
6	a= 8.765(4) b= 24.452(5) c= 20.640(3)	β=γ=90 α=106,57	monoclinic	P2/c	4	4239	2.636	2.490
7	a= 15.179(5) b= 19.644(8) c= 24.986(4)	α=β=γ=90	orthorhombic	$Pna2_1$	4	7450	1.516	1.480
9	a = 19.613(5) b = 12.242(7) c = 18.419(8)	α=88.766 β=93.669 γ=101.194	triclinic	$P\bar{1}$	2	1977	1.215	1.200
10	a = 21.357(5) b = 18.226(7) c = 8.213(5)	α=83.305 β= 90.660 γ= 93.623	triclinic	$P\bar{1}$	2	3160	1.500	1.380
12	a = 8.149(5) b = 44.448(9) c = 25.825(4)	α=β=γ=90	orthorhombic	Pbca	8	9350	2.656	2.499
13	a = 17.699(7) b = 8.542(4) c = 28.112(6)	β=γ=90 α=93.96	monoclinic	P2/c	4	4240	2.906	2.832
14	a = 8.224(6) b = 44.618(5) c = 25.549(6)	α=β=γ=90	orthorhombic	Pbca	8	9374	2.657	2.533

*Density was determined by picnometer method

The coordination polymers **16**, **18** and **19** are amorphes.

III.1.1.2. Characterization of the coordination polymers 5-7 by thermal gravimetric analysis-TGA.

Thermal gravimetric analysis of the compounds **5-7** are shown in **Figure 31-33**.

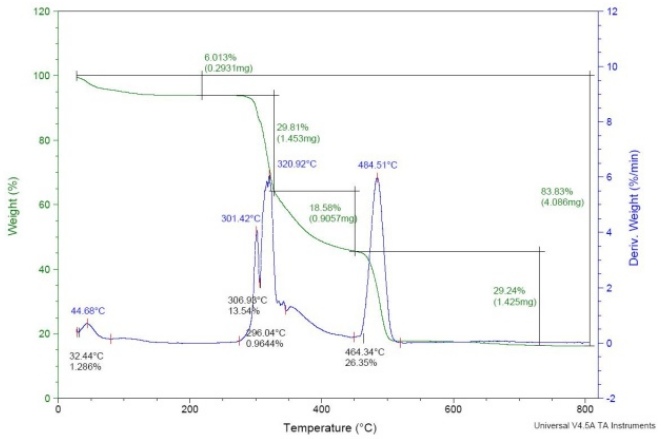

Figure 31. DSC-TGA curves for $[\{Cu(cyclam)\}_3(trt)_2 \cdot 6H_2O]_n$ (**5**)

DSC-TGA curves for **5** (see **Figure 31**) showed a lost of six guest water molecules at 44.68 °C succeeded by three consecutive weight losses in 301.42-484.51 °C range with the loss of the tartrazine trianion and of macrocyclic ligand. Finally, the CuO residue (observed 16.17%, calculated 13.27%) remained above 484.51 °C.

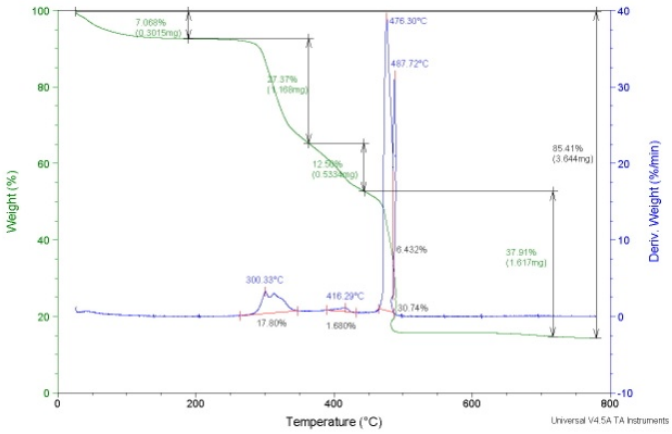

Figure 32. DSC-TGA curves for $[\{Ni(cyclam)\}_3(trt)_2 \cdot 43H_2O]_n$ (**6**).

DSC-TGA curves for **6** (see **Figure 32**) showed a first weight lost of solvent (approximately 43 water molecules) at 300.33 °C. According to literature data the lost of water molecules in 300-360 °C range correspond to loss of crystallization water.[134] On the further heating, three consecutive weight losses were observed in 416.29-487.72 °C range with the lost of azo dye and macrocyclic ligand. Finally the NiO residue (observed 14.32%, calculated 12.39%) remained above 487.72 °C.

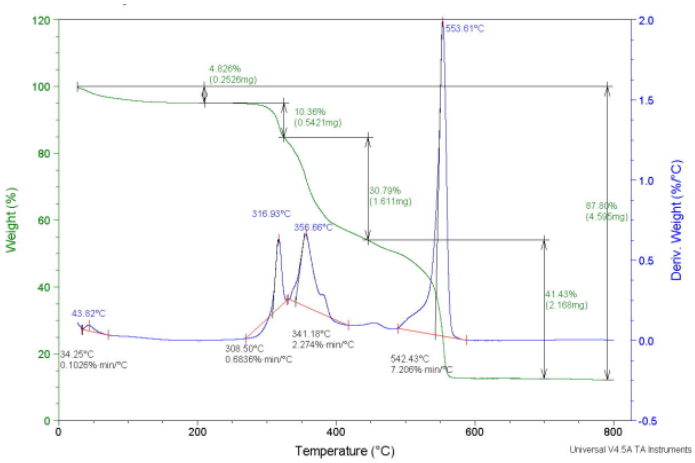

Figure 33. TGA curves for $[\{Zn(cyclam)\}_3(trt)_2 \cdot 5H_2O]_n$ (**7**).

DSC-TGA curves for **7** (see **Figure 33**) showed a first weight lost of five guest water molecules at 43.82 °C. On the further heating, three consecutive weight losses were observed in 316.71–551.48 °C range with the lost of azo dye and macrocyclic ligand. Finally the ZnO residue (observed 12.47%, calculated 12.48%) remained above 551.48 °C.

DSC-TGA analysis of the PC **9**, **10**, **12**-**14**, **16**, **18** and **19** allowed, in a similar manner to the above analysis for PC **5**-**7**, to estimate the amount of solvents and polymers present in the guest host, and the theoretical amount of oxide, comparison with the observed, a verification in addition to elemental analysis of PC correctness.

III.1.1.3. Characterization of the coordination polymers 5-7 by vibrational spectra analysis

Because the changes in the electron density are relatively low at the carbon atoms to which sulfonic group are substituted[135] and the participation of sulfur d orbital in the conjugated system is very low, the π contribution into C-S bond is practically negligible in aza dye compounds.[136] Due to this fact, the results obtained by Neica, in her dissertation thesis,[146] in connection with identification of Raman spectrum vibrations of tartrazine can be applied in analysis of the similar spectra of the coordination polymer **5**-**7** (see **Figure 34**).

Thus, the very strong band at 1598 cm^{-1} for **5** and at 1597 cm^{-1} for **6** and **7** and the very weak at 1685cm^{-1} for **5**, and 1691cm^{-1} for **6** and **7** were attributed to the C=C symmetrical stretching mode of pyrazole mixed with quadrant stretching mode of the phenyl rings contribution, and with C-H bending mode of OH group, respectively. The bands at 1501s, 1474m, 1411w cm^{-1} for **5**, at 1502s, 1475m, 1409w cm^{-1} for **6**, and at 1506s, 1475m, 1410w cm^{-1} for **7** were attributed

to C=C pyrazole bending contribution mixed wirh the N=N bending mode, and with the C-H bending mode of the phenyl ring contribution.

The strong band at 1339 cm^{-1} for **5**, 1333 cm^{-1} for **6** and **7** is due to the azo group stretching mode (C-N=N-C) mixed with the symmetrical stretching of carboxyl group. The very weak band at 1268 cm^{-1} for **5**, at 1266 cm^{-1} for **6**, and at 1267 cm^{-1} for **7** was assigned to the bending mode of (N-N=C-$C_{carboxylic}$) moiety from pyrazole ring. The medium strong band at 1216 cm^{-1} for **5**, 1214 cm^{-1} for **6**, and at 1215 cm^{-1} for **7** was assigned to the C-H torsion mode of both phenyl rings, to the N=C-$C_{carboxylic}$ moiety bending mode, and to the stretching mode of C_{phenyl}-N and $C_{pyrazol}$-N (N belong to the azo group). The strong band at 1121 cm^{-1} for **5**, **6** and **7** corresponds to the out-of-plane C-H deformation of the phenyl rings.

The next band at 1087 cm^{-1} for **5**, at 1088 cm^{-1} for **6** and at 1089 cm^{-1} for **7** corresponds to the phenyl bending mode bonded by nitrogen of pyrazole ring. The band at 1032 cm^{-1} for **5** and **7**, and at 1042 cm^{-1} for **6** was attributed to the phenyl bonded by azo group bending mode, to the N=N asymmetrical mode and to the C-SO_3^- symmetrical stretching mode. The very weak band observed at 1010 cm^{-1} for **5** and **7**, and at 1008 cm^{-1} for **6**, correspond to the C-H out of plane deformation mode of phenyl bonded by azo group. The very weak peak at 867 cm^{-1} for **5**, at 871 cm^{-1} for **6** and at 869 cm^{-1} for **7** can be attributed to the out-of-plane deformation of both phenyl rings, and to the bending modes of hydroxyl and carboxyl groups.

The bending mode of SO_3^- group substituted on phenyl moiety bonded by pyrazole appears as weak band at 803 cm^{-1} for **5**, and at 805 cm^{-1} for **6** and **7**. The very weak band at 764 cm^{-1} for **5**, at 767 cm^{-1} for **6**, and at 764 cm^{-1} for **7** was assigned to the bending mode of SO_3^- group from phenyl moiety bonded by azo group and to the out of plane C-H deformation of phenyl group bonded by azo group. The very weak peak at 712 cm^{-1} for **5** and **7**, and at 715 cm^{-1} for **6** appears due to the bending modes of both SO_3^- groups. The medium strong band at 693 cm^{-1} for **5**, and at 694 cm^{-1} for **6** and **7** was assigned to out-of-plane CH deformation of pyrazole ring. The medium intensity signal at 634 cm^{-1} for **5**, and at 636 cm^{-1} for **6** and 7 represents the out-of-plane deformation of phenyl rings, and the medium intensity signal at 609 cm^{-1} for **5** and **7**, and at 611 cm^{-1} for **6** can be assigned to the pyrazole bending, and to the out-of-plane CH deformation of the phenyl rings. The very weak band at 511 cm^{-1} for **5**, at 510 cm^{-1} for **6**, and at 509 cm^{-1} for **7** represents the wagging mode of SO_3^- group substituted on phenyl moiety bonded by pyrazole, and out-of-plane C-H deformation of phenyl and pyrazole rings. The medium band observed at 484 cm^{-1} for **5** and **6**, and at 483 cm^{-1} for **7** can be attributed to a skeletal distortion and to the both sulfonate groups rocking modes.

The theoretical calculation[137] showed that the azo distance for tartrazine molecule is 127.1 pm. The calculated N=N bond distance is 124.5-125.0 pm for OH tautomer whereas the N-N bond distance for NH isomer is 130.0 pm.[138] The bond length between nitrogen and C of pyrazole ring, with OH substituent is 136.5 pm, which is shorter then that between azo N and the C of the phenyl ring 142.1 pm.[44,139] The elongation of the bond length supports the charge delocalization from

pyrazole ring and the localization at the azo bond.[140,141,155] The calculated C=C bond lengths of the pyrazole ring vary from 140.2 to 140.5, which is between the length of a C-C single bond (154.0 pm) and that of a C=C double bond (134.0 pm).[137,142]

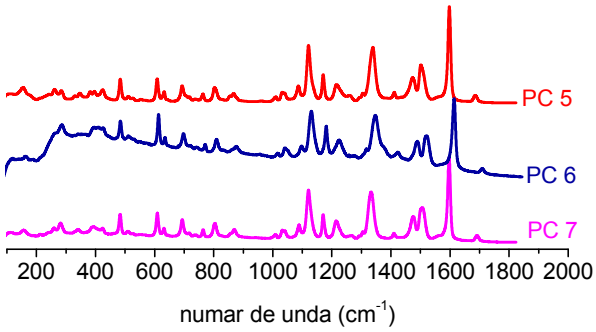

Figure 34. Experimental Raman spectra recorded in solid state of the compounds $[\{Cu(cyclam)\}_3(trt)_2\cdot 6H_2O]_n$ (**5**), $[\{Ni(cyclam)\}_3(trt)_2\cdot 43H_2O]_n$ (**6**) and $[\{Zn(cyclam)\}_3(trt)_2\cdot 5H_2O]_n$ (**7**).

Similarly, the calculated C=N bond length from pyrazole ring vary from 135.0 pm to 137.7 pm, lengths which are also intermediate between those for a C-N single bond (148.0 pm) and C=N double bond (128.0 pm).[48,137] The calculated data suggest an extended π delocalization over the pyrazole system.[49,143] Due to this density electron donation a decreasing of the bond order of the azo group and lengthening of the bond take place, indicating the presence of NH tautomer in solid tartrazine. This electronic delocalization take also place and in coordination polymers, where the tartrazine trianion is coordinated by transitional metals, and the NH tautomer is present in the solid form (*vide infra*).

For analysis of the IR spectra of compounds **5**-**7** (see **Figure 34**) we have taken into consideration theoretical calculations of these spectra of other azo dyes from literature.[144,145,147a,161]

Thus cyclam moiety from these compounds display in the infrared spectrum two medium strong bands at 3229, 3168 cm^{-1} (for **5**), 3262, 3214 cm^{-1} (for **6**) and 3255 cm^{-1} (for **7**) corresponding to the N-H stretching, two medium strong bands at 2935 cm^{-1} and 2873 cm^{-1} (for **5**) at 2926 cm^{-1} and 2864 cm^{-1} (for **6**) and at 2925 cm^{-1} and 2869 cm^{-1} (for **7**) corresponding to CH_2 asymmetric and symmetric stretching, respectively.

The in-plane OH deformation vibration appears in the IR as strong band at 1475 cm^{-1} (for **5** and **6)** and at 1476 cm^{-1} (for **7**) corresponding to in-plane-bending vibration of OH group.[144] The OH out-of plane deformation vibration in the IR lies in the region 290-320 cm^{-1} for free OH and in the region 517-717 cm^{-1} for associated OH.[144]

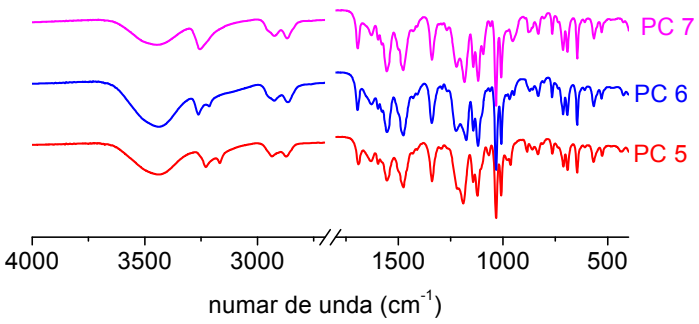

Figure 35. Experimental infrared spectra recorded in solid state of the compounds: $[\{Cu(cyclam)\}_3(trt)_2\cdot 6H_2O]_n$ (**5**), $[\{Ni(cyclam)\}_3(trt)_2\cdot 43H_2O]_n$ (**6**) and $[\{Zn(cyclam)\}_3(trt)_2\cdot 5H_2O]_n$ (**7**).

The medium strong band at 711 cm^{-1} (for **5**), at 713 cm^{-1} (for **6** and **7**) in the IR spectra corresponds to out-of-plane bending mode of hydroxyl vibrations.

Asymmetric vibrations of SO_3^- group of sulfonic acid salts usually occur in the IR at 1250-1140 cm^{-1}.[136] The band due to the symmetric stretching vibration is sharper and occurs at 1130-1080 cm^{-1}. SO_3^- symmetric deformation modes give strong bands in the 550-660 cm^{-1} region (IR).[146,147] The asymmetric stretching mode of SO_3^- is mixed with C-N stretching, C-H in-plane-bending[136] giving a very intense band at 1190 cm^{-1} for **5**, at 1175 cm^{-1} for **6** and at 1184 cm^{-1} for **7**. The very intense band at 1033 cm^{-1} for **5**-**7** in the IR can be attributed to symmetric stretching vibrations of SO_3^- group.[144] SO_3^- symmetric bending vibrations produce a weak intense band at 764 cm^{-1} for **5**, at 766 cm^{-1} for **6**, and at 765 cm^{-1} for **7** and a medium one at 691 cm^{-1} for **5**, at 692 cm^{-1} for **6** and **7** in the IR. The weak IR band at 527 cm^{-1} for **5**, at 528 cm^{-1} for **6** and **7** and weak band at 435 cm^{-1} for **5**, at 424 cm^{-1} for **6** and at 425 cm^{-1} for **7** correspond to SO_3^- wagging vibrations.

The asymmetric vibrations of COO^- group appear as a strong band at 1554 cm^{-1} for **5**, and for **6**, and at 1555 cm^{-1} for **7**. The symmetric vibrations of the same group produce a strong band at 1338 cm^{-1} for **5**, at 1340 cm^{-1} for **6**, and at 1339 cm^{-1} for **7**.

The difference ($\Delta\nu$) between symmetric and asymmetric vibrations of the carboxylate groups in the case of compound 5 and 7 is 216 $cm^{-1}$and 214 for 6, and only 83 for tartrazine (Na_3trt), difference which sustain an monodentate coordination mode.[174]

N=N stretching vibrations, due to its symmetry, has a very characteristic band in the Raman spectroscopy but are difficult to observe in the IR spectrum. The change of N=N bond length in the molecule which has two unequivalent C-N parts (*vide supra*) produces a modification in the dipole moment. Due to this effect the N=N stretching mode became active in the IR and has a medium intensity. The band occurring between 1450 cm^{-1} and 1380 cm^{-1} correspond to the stretching mode of an azo-compound.[148] C-N stretching vibrations of azo-compounds appear in the 1200-1130 cm^{-1} region (IR).[149,150] The strong band at 1220 cm^{-1} (sh) for **5,** at 1223 cm^{-1} for **6** and at 1221 cm^{-1} for **7**

in the IR spectrum can be attributed to the azo stretching vibrations. This large downshift of these vibrations can be explained by a greater conjugation and by a π-electron delocalization.[163,165]
The weak intensity band at 1293 cm^{-1} for **5,** at 1291 cm^{-1} for **6** and **7** in the IR, originate from the stretching mode of C-N.[152] The (C-N=N-C) chromophore gives a very intense band at 1009 cm^{-1} for **5** and **7**, and at 1008 $cm^{-1}$for **6**.[144] Oliveira and coworker[147a] predicted for the NH isomer, quite intense bands at 1554, 1324, and at 1294 cm^{-1}.

The first absorption was assigned as a combined mode including δNH, νCO, νC=N, βCH vibrations, and the other two bands are attributed to δNH, νN-H, βCH, νCC modes. All of these vibrations are characteristic for keto-hydrazo isomer and may be used as fingerprints in the IR spectrum. Oliveira observed experimentally, in the case of azo dye Ponceau 4R, only two bands at 1495 and at 1221 cm^{-1}. In the IR spectra of compounds **5**-**7** these vibrations were identified, as strong bands, at 1554 cm^{-1} for **5** and **7**, at 1555 $cm^{-1}$for **6** and at 1220 cm^{-1} (sh) for **5,** at 1223 cm^{-1} for **6** and at 1221 cm^{-1} for **7**. The bands from 1220-1223 cm^{-1} range are mixed with azo stretching vibrations (*vide supra*).

As in case of Raman spectra, the IR vibrations are mixed with vibrations produced by phenyl and pyrazole rings.[151,153]

Because that all prepared coordination polymers **9**, **10**, **12**-**14** and **16** have the same kind of substituents (see **Figure 1**), their vibrations in the IR and Raman spectra, appear in the same region as those of the polymers **5**-**7,** discuted in the details previously. In the case of polymers **18** and **19** two amino groups appear as substituents on naphthalene rings, but because these substituents are in symmetric position as compared to azo group, the asymmetry of the molecule disapeared. As a result, the dipolmoment that determine appearence of azo group vibrations in IR canceled and these vibrations became inactive.

III.2 CARBOXYLATE COORDINATION POLYMERS

III.2.1. SYNTHESIS OF THE COORDINATION POLYMERS $[Cu(cyclam)(tart)\cdot 7H_2O]_n$ (21), $[Ni(cyclam)(tart)\cdot 5H_2O]_n$ (22) AND $[Ni(cyclam)(ox)\cdot 2DMF\cdot 8H_2O]_n$ (24).

Coordination polymers that contain $[M(cyclam)(ClO_4)_2]$ (M = Ni^{2+}, Cu^{2+}, Zn^{2+}) and aliphatic or aromatic carboxilates namely: sodiu and potasium tartrate, ammonium oxalate and sodium fumarate. In this way the following PC were obtained: $[Cu(cyclam)(tart)\cdot 7H_2O]_n$ (**21**). $[Ni(cyclam)(tart)\cdot 5H_2O]_n$ (**22**) and {$[Ni(cyclam)(ox)\cdot 2DMF\cdot 8H_2O]_n$ (**24**) were prepared. Another PC from the same type $[Cu(hatco)]_2$ [tcm]$\cdot 11H_2O$ (**30**) were obtained by complexation of $[Cu^{2+}(hatco)(ClO_4)_2]$ of (**29**) with Na_4tcm (**28**).

III.2.1.1. Characterization of the coordination polymers 21, 22 and 24 using powder X-ray diffraction.

The growth of the single-crystal in the case of compounds PC **21**, **22** and **24** failed, so we characterized them, from crystallographic point of view, by means of the powder XRD spectra. The crystal data for these coordination polymers are shown in **Table 15**.

Table 15. Crystal data for coordination polymers PC **21**, **22** and **24.**

PC	Elementary lattice		Crystal system	Space group	Z	Volume Å^3	$\rho_{calc.}$ g·cm^{-3}	$\rho_{det.}$* g·cm^{-3}
	Å	Grade						
21	a= 8.765(6) b= 24.452(2) c= 20.640(3)	$\beta=\gamma=90$ $\alpha=100.56$	monoclinic	$P2_1/c$	4	2000	1.373	1.233
22	a= 15.195(7) b= 19.730(2) c= 24.735(4)	$\alpha=91.21$ $\beta=98.70$ $\gamma=98.81$	triclinic	$P\bar{1}$	4	590.5	2.290	2.091
24	a = 12.244(5) b = 15.545(8) c = 17.733(4)	$\beta=\gamma=90$ $\alpha=92.62$	monoclinic	$P2_1/c$	4	1397	1.656	1.499

*Density was determined by picnometer method

III.2.1.2. Characterization of the coordination polymers 21, 22 and 24 by thermal gravimetric analysis-TGA

Thermogravimetric analyses of the compounds **21** şi **22** are presented in **Figures 64** şi **65**.

DSC-TGA curves for $[Cu(cyclam)(tart)\cdot 7H_2O]_n$ (**21**), (see **Figure 64**) showed a lost of seven guest water molecules in the temperature interval of 35.56-91.22 ºC, centered at 78.76 ºC. At further heating, four consecutive weight losses in 222.50–331.84 ºC range are produced, with the loss of tartrate dianion and of macrocyclic ligand. Finally, the CuO residue (observed 20.09%, calculated 19.31%) remained above 331.84 °C.

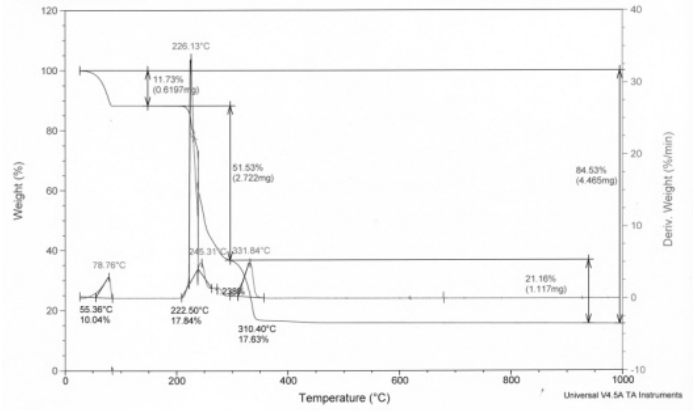

Figure 64. DSC-TGA curves for $[Cu(cyclam)(tart)\cdot 7H_2O]_n$ (**21**)

DSC-TGA curves for $[Ni(cyclam)(tart)\cdot 5H_2O]_n$ (**22**), (see **Figure 65**) showed a lost of five guest water molecules in the temperature interval of 47.73-71.22 ºC, centered at 58.90 ºC. At further heating, four consecutive weight losses in 231.89–401.01 ºC range are produced, with the loss of tartrate dianion and of macrocyclic ligand. Finally, the NiO residue (observed 18.07%, calculated 18.35%,) remained above 401.01 ºC.

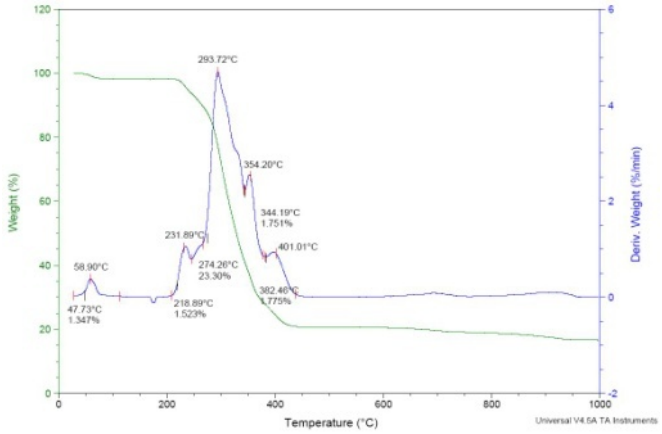

Figure 65. DSC-TGA curves for $[Ni(cyclam)(tart)\cdot 5H_2O]_n$ (**22**)

The thermogravimetric analysis of compound **24** is presented in **Figure 66**. DSC-TGA curves for $[Ni(cyclam)(ox)\cdot 2DMF\cdot 8H_2O]_n$ (**24**) showed a lost of nine guest water molecules in the temperature ranges of 30.72-59.43 ºC, centered at 41.33 ºC, and of 59.43-102.33 ºC, centered at 76.06 ºC. At further heating, two DMF molecules are lost in 177.38–249.503 ºC range, centered at 200.88 ºC. In the range 319.54-365.11 ºC two weight losses coresponding to oxalate dianion and of macrocyclic ligand are produced. Finally, the NiO residue (observed 22.33%,calculated 21.52%,) remained above 365.11 ºC.

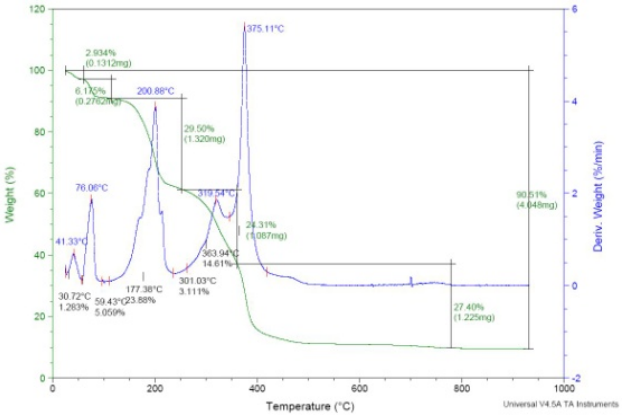

Figure 66. DSC-TGA curves for $[Ni(cyclam)(ox)\cdot 2DMF\cdot 8H_2O]_n$ (**24**)

III.2.1.3. Characterization of the coordination polymers 21, 22 and 24 by the analysis of IR vibrational spectra.

The difference ($\Delta\nu$) between symmetric and asymmetric vibrations of the carboxylate can be used for the determination of the mode through which the carboxylate group of polymer incoordinates the metal. The carboxylate ion is able to coordinate the metals in three ways: [174]

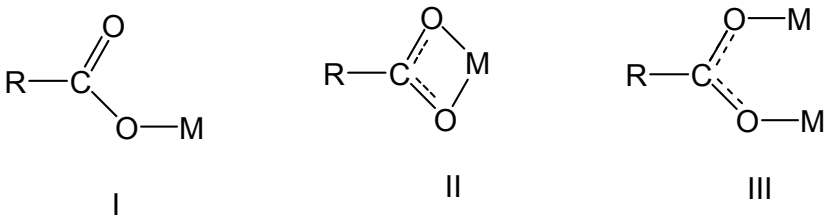

- the monodentate complexe (structure I) has a much higher $\Delta\nu$ value than the ionic compound.
- the chelate complexe or bidentate (structure II) has a smaller $\Delta\nu$ value than the ionic compound.
- the bridging complexe (structure III), that has a C_2 axial symmetry, has a $\Delta\nu$ value close to that of the ionic compound.

From IR spectra analyses, in solid state, of the polymers **21** and **22** (see **Figure 67**), result that $[Cu(cyclam)(tart)\cdot 7H_2O]_n$ (**21**) has the structure of the monodentate complexe, $\Delta\nu$ difference being 274 cm^{-1} (νCOO^-_{as}=1604 cm^{-1}, νCOO^-_s =1330 cm^{-1}) and in the ionic compound this difference is equal with 213 cm^{-1} (νCOO^-_{as}=1603 cm^{-1}, νCOO^-_s=1390 cm^{-1}). $[Ni(cyclam)(tart)\cdot 5H_2O]_n$ (**22**) shows the same structure, the difference $\Delta\nu$ of the polymer being 251 cm^{-1} (νCOO^-_{as}=1604 cm^{-1}, νCOO^-_s=1353 cm^{-1}).

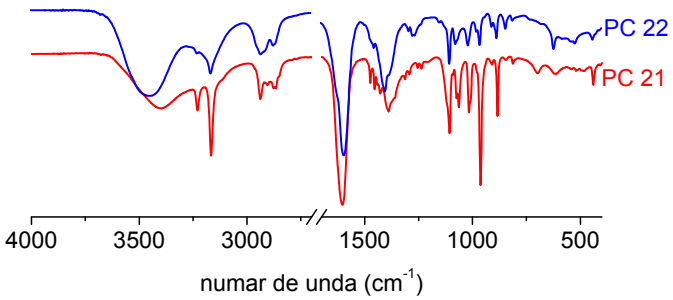

Figure 67. The IR spectra of CP **21** and **22**

III.2.2. SYNTHESIS OF THE COORDINATION POLYMERS [{Cu(cyclam)(H$_2$O)$_2$}(fum)·4H$_2$O]$_n$ (26) AND [{Ni(cyclam)(H$_2$O)$_2$}(fum)·4H$_2$O]$_n$ (27)

Reaction of [Cu^{2+}(cyclam)](ClO$_4$)$_2$ (**2**) and [Ni^{2+} (cyclam)](ClO$_4$)$_2$ (**4**), in DMF, with sodium fumarate (**25**), in water, gives coordination polymers [{Cu(cyclam)(H$_2$O)$_2$}(fum)·4H$_2$O]$_n$ (**26**) and [{Ni(cyclam)(H$_2$O)$_2$}(fum)·4H$_2$O]$_n$ (**27**), according to the **Schemes 36** and **37**.

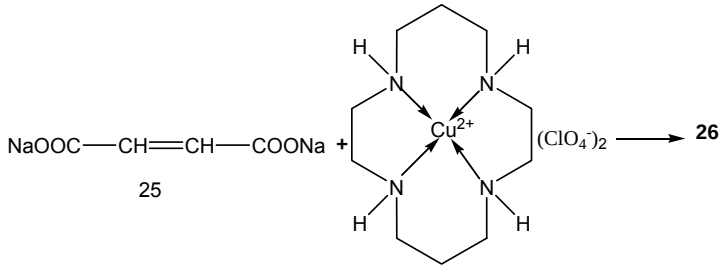

Scheme 36. Synthesis of the compound [{Cu(cyclam)(H$_2$O)$_2$}(fum)·4H$_2$O]$_n$

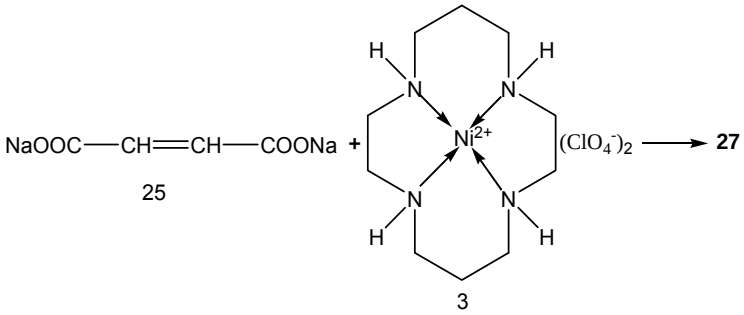

Scheme 37 Synthesis of the compound [{Ni(cyclam)(H$_2$O)$_2$}(fum)·4H$_2$O]$_n$ (**27**)

III.2.2.3. Molecular and crystalline structure of the coordination polymers 26 and 27 determined by X ray monocrystal diffraction

In complex cations, metal atom has a distorted octahedron coordination geometry. Ecuatorial positions are occupied by 4 nitrogen atoms belonging to the macrocyclic ligand, and in the axial positons, the metal atom is coordinated by the water molecules (see **Figure 71**).

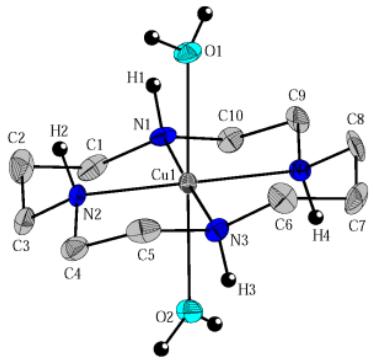

Figure 71. ORTEP diagram of the complex cation $[Cu(cyclam)(H_2O)_2]^{2+}$ of **26**

The length of bonds Cu-N [2.010(7) – 2.024(9) Å is similar with the interatomic distances Cu-N observed in the similar cation of $[Cu(cyclam)(H_2O)_2](OAc)_2 \cdot 2MeOH$ [2.012(2) / 2.018(2) Å][221] or in the coordination polymer $[Cu(cyclam)\{H_2(1,2,4,5\text{-btetc})\} \cdot H_2O]_n$ [2.006(2) – 2.032(2) Å][94] in which the copper atom is coordinated by the same azamacrocyclic compound.

The coordination of Cu^{2+} by the water molecules in the complexe **26** [Cu(1)–O(1) 2.456(9) Å, Cu(1)–O(2) 2.428(6) Å], instead of the organic acid anion shows a behaviour often met in the case in which the water presence is not avoided, for example in case of $[Cu(cyclam)(H_2O)_2](OAc)_2 \cdot 2MeOH$,[221] or $[Cu(cyclam)(H_2O)_2](OOCC_6H_4\text{-}Bu^t)_2$.[222] A similar phenomenon can be observed in the case of $[Cu(dap)_2(H_2O)_2]$(naftalin-1,5-disulfonat)$\cdot 2H_2O$ and $[Cu(N,N'\text{-men})_2(H_2O)_2]$(naftalin-1,5-disulfonat)$\cdot H_2O$ (where dap = 2,3-diaminopropane; N,N'-men = N,N'-dimethylethylendiamine), complexes, where the SO_3^- large group can not draw near to the Cu^{2+} due to some steric reasons.[138]

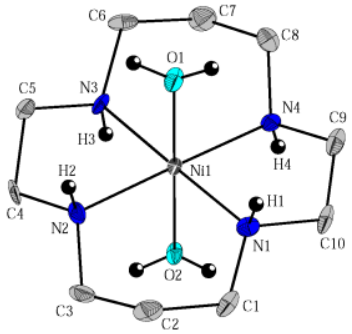

Figure 72. ORTEP diagram of the complexe cation $[Ni(cyclam)(H_2O)_2]^{2+}$ from complex **27**.

Similar considerations are valid in the case of complex cation **27** (**Figure 72**), where the Ni-N distances [2.042(6) – 2.084(6) Å] are comparable with those observed in the similar cations of $[Ni(cyclam)(H_2O)_2]Cl_2 \cdot 4H_2O$ [2.065(3) / 2.072(2) Å][223] or $[Ni(cyclam)(H_2O)_2]_3(1,3,5\text{-btc})_2 \cdot 24H_2O$ [2.057(3) / 2.069(4) Å] compounds.[54]

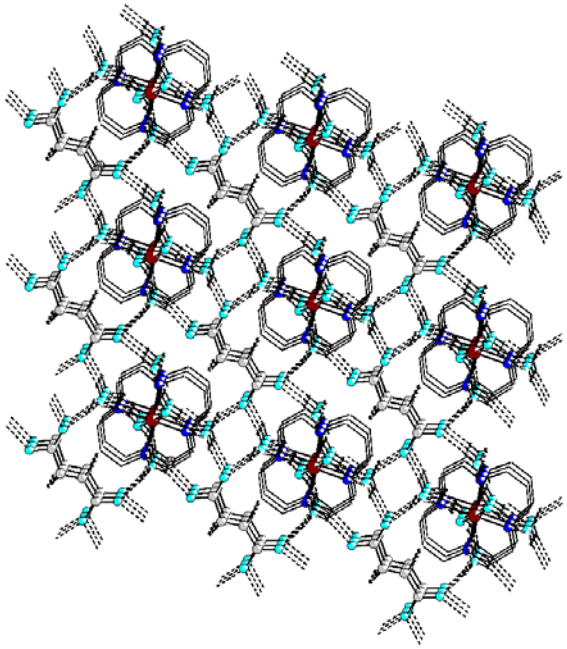

Figure 73. 3D network created by hydrogen bonds in the crystal of the complex **26**
[C - gray, O - cyan, N - blue, Cu^{2+} - brown, H – black]

A carefully examination of the compound **26** crystal reveals a hydrogen bond complexe network / oxygen-hydrogen contacts (shorter than the sum of van der Waals radii (Σr_{vdW}(O,H) 2.60 Å),[225] which involve the fumarate anion, water molecules and hydrogen atoms belonging to the nitrogen atoms of the cyclam macrocycle. (**Figure 73**).

III.2.3. SYNTHESIS OF THE COORDINATION POLYMER $[\{Cu(hatco)\}_2(tcm)\cdot 11H_2O]_n$ (30)

Self-assembling reactions of $Cu(hatco)(ClO_4)_2$ with Na_4tcm in DMF/H_2O (1:1, v/v) give the coordination polymer $[\{Cu(hatco)\}_2(tcm)\cdot 11H_2O]$ (**30**) depicted in the **Scheme 38.**

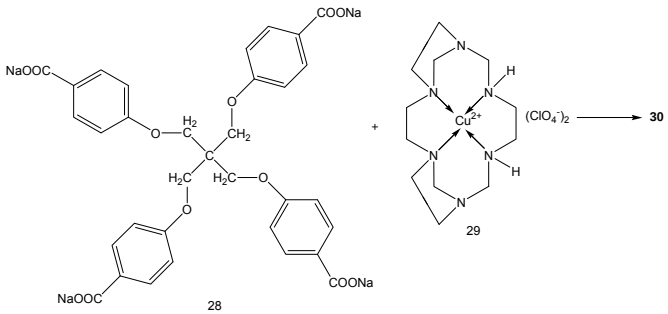

Scheme 38. Synthesis of the polymer $[\{Cu(hatco)\}_2(tcm)\cdot 11H_2O]$ (**30**)

III.2.3.3. Molecular and crystalline structure of the coordination polymer 30 determined by X ray monocrystal diffraction

Among the six nitrogen atoms of the macrocycle, only four are coordinated at the metal atom (**Figure 76**), giving an ecuatorial plane belonging to a very distorted octahedron with axial positions occupied by the oxigen atoms from two different organic anions.

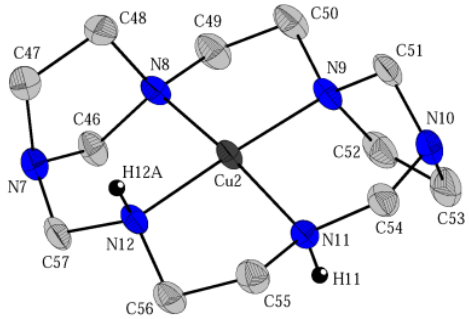

Figure 76. ORTEP diagram of the fragment $[Cu(HATCO)]^{2+}$ from complex **30**.

The bond lengths Cu-N [2.002(4) – 2.032(4) Å] are similar with the interatomic distances Cu-N observed in the molecular complex $[Cu(HATCO)]_2[Mo(CN)_8]\cdot H_2O$ [1.992(5) – 2.036(8) Å] [227] in which the copper atom is coordinated by the same macrocycle. We can notice an accented asymmetry of the Cu-O bond length from the axial position in the case of the both independent octahedron fragments: Cu(1)–O(2) 2.304(3) Å / Cu(1)–O(12) 3.489(3) Å, respectivelly Cu(2)–O(5) 2.300(3) Å / Cu(2)–O(9) 3.046(4) Å.

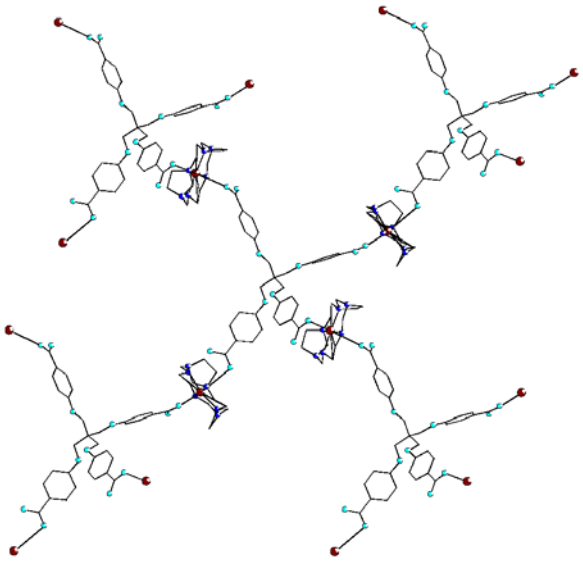

Figure 77. 3D network created in the crystal of 3D coordination polymer **30**
[C - gray, O - cyan, N - blue, Cu^{2+} - brown]

Tetrametallic bridging coordination of the organic acid tetraanion has been met in the case of $[Ni_4(cyclam)_4(TCM)_2 \cdot 4DMF \cdot 20H_2O]_n$ coordination polymer.[99] Surprinsing, though carboxylato groups are coordinated by only one oxygen atom to copper atom, the carbon-oxygen bond lengths in the $-CO_2^-$ unit are similar, this fact suggesting an accented delocalization of the negative charge. An explanation, could be the achievement of some strong hydrogen bonds in which the water molecules are involved. Unfortunatelly, the disorder at the level of those molecules in the coordination polymer **30,** hinders a detailed study of the 3D network in which are involved the hydrogen bonds of the water molecules. In the **Figure 77** it is shown the 3D network created in the crystal of 3D coordination polymer **30**

III.4.3. Porosity and specific surface characterization of the synthetized sulfonate coordination polymers

From the specific surface measurements it resulted that only four sulfonate azo- dye coordination polymers (**CP 9**, **10**, **13**, **14)** from the 11 prepared, show porosity**.** In the following the characterization of porosity and specific surface of CP **13** (see **Figure 88**) is presented. The nitrogen adsorption isotherms of the studied samples were measured by volume of adsorbed gases at 77K after degassing at 200 °C for three hours. Porosity of the coordination polymer $[\{Ni(cyclam)\}_3(amrt)_2 \cdot 4H_2O]_n$ (**13**) was studied through N_2 adsorption-desorption by volumetric method. Adsorption-desorption isotherms shown in **Figure 88** are of type I (Langmuir), characterized by a steep slope in p/p_0 relatively low domain, followed by a plateau due to filling of micropores.

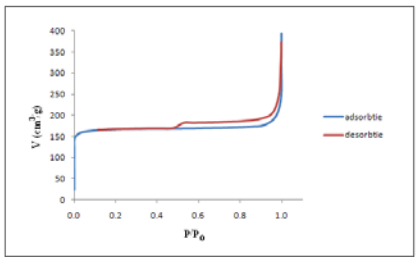

Figure 88. Adsorption-desorption isotherm of N_2 for the coordination polymer **13**.

These isotherms show a H_4 type hysteresis, characteristic of microporous adsorbent with long and slit shaped pores.[184] Hysteresis loop of H_4 type is closed to an equilibrium pressure near to the saturation pressure. In such situations, it seems that, the position of the desorption isotherm depends on the maximum pressure reached before starting desorption. From the physisorption

data, the values of 626 m^2/g for S_{BET}, 736 m^2/g for S_L and 0.38 cm^3 /g for the specific volume of pores were obtained.

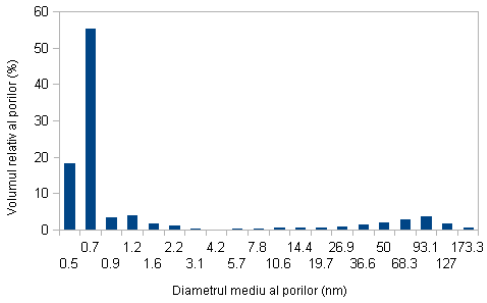

Figura 89. Distribution of pores in the coordination polymer **13.**

Distribution of pores in the coordination polymer **13**, presented in the plot of **Figure 89** shows that 84% of the pores have dimensions in the microporous range. The smaller are the pore sizes, the higher is the adsorption energy because the neighborhood walls adsorbent increases adsorbate/adsorbent interactions, decreasing also the relative pressure at which their filling up take place.

III.5. CHARACTERIZATION OF HUMIDITY SENSOR PROPERTIES OF SOME SYNTETIZED COORDINATION POLYMERS

In literature, a few studies about the humidity sensor using organic semiconductor have been presented. Investigations related to the colorant orange (Orange Dye, OD), a p-type organic semiconductor, for application as humidity sensor were achieved by Moiz and cowork.[208,209] Methyl red was another dye, that has been studied as a humidity sensor, using a cell formed from Ag/ methyl red / Ag.[210] These dyes are soluble in water and cannot be used to detect high concentrations of water. Nickel phthalocyanine, was also studied as humidity sensor.[211] It is insoluble in water and thermally stable, and can be deposited in thin film by heat evaporation without dissociation.[212,213]

Encouraged by these results we tried to see if coordination polymers with azo dyes may show such properties. From all the polymers studied only one polymer, $[\{Cu(cyclam)\}_3(trt)_3 \cdot 6H_2O]_n$ (**5**), that is similar to nickel phthalocyanine because is practically insoluble in water, presented properties that recommend it for use as humidity sensor.

The polymer $[\{Cu(cyclam)\}_3(trt)_3 \cdot 6H_2O]_n$ **5** was pastillated, at a pressure of 100 atm. with a device commonly used in IR and Raman preparation of samples, in cylindrical form with a diameter of 10 mm and thickness of 0.3 mm. After this treatment there were no structural changes observed in the structure of the polymer **5**. This fact was confirmed by analyses of X diffraction, IR and Raman spectra. In order to measure conductivity properties of this polymer (accepting a priori that

it shows isotropy in volume phase of the pastille) the variation of the pastille resistance with temperature in -130°C +19°C temperature range was studied.

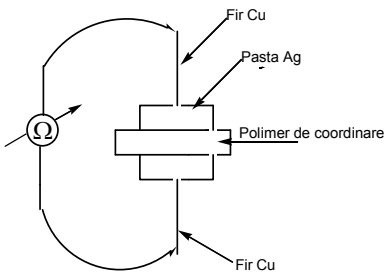

Figure 98

On circular surfaces of the pastille, the wires Cu conductors with low specific resistance with Ag conductive paste were sticked (see **Figure 98**). After this stage the socked remained in the oven at room temperature for 72 hours. This time was needed to achieve the strengthening of the connections and to avoid a massive migration of Ag ions in the substrate structure. Resistance and temperature measurements were made using an electronic multimeter UT60 connected to computer. Have to specify that the temperature sensor was attached to the sample pellet at the interface metal (Ag) / organic compound.

The sample was initially immersed in liquid nitrogen and then extracted from it and exposed to the laboratory atmosphere. No connections damage or cracks in the sample were observed. In the preliminary determinations, in the absence of the thermostability at low temperatures, the experiments pursued the temperature modification in the course of time on contact surface of the sample and the variation in time of the sample resistance in immersion and in the laboratory atmosphere. From these data the dependence of sample resistance in function of the temperature were configured.

Analyzing the temperature / time dependence is observed that there is a rapid temperature change of the interface metal / organic compound, immediately after drawing of the sample from liquid nitrogen and exposure to laboratory atmosphere, time in which this change occurs, although is short, does not affect the sample. The phenomenon is reversible during the sample immersion in the liquid nitrogen. Sample undergoes a dramatic resistance change of the value from 150 MΩ to 1.98 MΩ in the interval in which the transition temperature of liquid nitrogen to the laboratory environment take place, inițial (12 s), after that follows a relatively slow growth (500 s) of the sample resistance up to the value of 60 MΩ followed by a quick return (15 s) to the value of 150 MΩ.

Dramatic changes of the resistance occur between (-10°C, +20°C) around the value of 0°C, and 18°C, respectively, the characteristic of the resistance-temperature having a step function form in the first temperature range. Visual inspection of the sample during the experiments revealed the

occurrence of condenses, that in our opinion would be, probable, due to the presence of the moisture in the laboratory atmosphere.

In usually way, the sample conductivity at room temperature can be explained by concerted contribution given by the resistance of organic compound crystallites and that of the intercrystallite barriers. Evidently, resistance of the barriers at the level of crystallite contacts has a much higher value than that of the crystallites, fact that explain the high resistance of the sample to continue electric current measurements. Dramatic changes of the resistance around the value of 0°C might be due to the fact that resistance of intercrystallite barriers is much lowered by the presence of water molecules. Conductivity of the sample is thus, due to both the temperature variations and barriers intercrystallite variation (variation managed by humidity)

Step-type behavior of the sample to the temperature changes, in the mentioned interval, could serve to construction of some functional electronic devices for humidity detection at tens of degree temperatures around the value of 0°C.

IV. CONCLUSIONS

1. Seventeen new coordination polymers (**5**, **6**, **7**, **9**, **10**, **12**, **13**, **14**, **16**, **18**, **19**, **21**, **22**, **24**, **26**, **27** and **30**) using as starting materials [M(cyclam)(ClO_4)$_2$] (M = Ni^{2+}, Cu^{2+}, Zn^{2+}; cyclam = 1,4,8,11-tetraazacyclotetradecane), [Cu(hatco)(ClO_4)$_2$] (hatco = 1,3,6,8,11,14-hexaazatricyclooctadecane), sulphonated azo dyes and aliphatic or aromatic carboxylates were obtained.

2. Sulphonated azo dyes coordination polymers (**5-7, 9, 10, 12-14, 16, 18, 19**) exhibit poor crystal growth properties, from this reason the single crystals were not obtained, and their crystal structure data were determined by means of powder X-ray diffraction. All sulphonated azo dyes coordination polymers are crystalline, excepting compounds **16, 18**, **19** that are amorphous. In the case of carboxylate coordination polymers **26**, **27** and **30** single crystals were obtained, but for the coordination polymers **21**, **22** and **24,** because the sigle cristal growth failed, the crystal structures were also determined by powder X-ray diffraction.

3. All new prepared coordination polymers were analyzed by TGA-DSC method. By this method was possible to make difference between guest and crystalization water molecules in the crystal.

4. Due to symmetry, N=N stretching has a very characteristic and intense Raman band but is difficult to observe in the IR spectra. When the sulphonated azo-dye coordination polymers is unsymmetrical substituted (**5**, **6**, **7**, **9**, **10**, **12**, **13**, **14**, **16**, **21**, **22**) i.e., just one aromatic ring is OH- or NH- substituted, a change in N=N bond length produces a change in the dipolmoment, making the IR mode active with medium intensity. The intense band observed at about 1360 cm^{-1} in the Raman spectra and the weak band at about 1366 cm^{-1}in the IR spectra can be attributed to the azo stretch. The azo stretch appears, in normal way, between 1380-1450 cm^{-1}. This large shift that is observed in the case of sulphonate azo dye coordination polymers can be explained by a greater conjugation and π-electron delocalization over the aromatic azo system, which is responsible for the molecules nonlinearity. When the sulphonate azo dye coordination polymers are symmetrically substituted (**18**, **19**) the change of the dipolmoment don't take place and as a result the IR mode became inactive.

5. The analysis of the IR and Raman spectra support the presence of the NH form in sulphonate azo dye coordination polymers, and the keto-hydrazone tauomer is mixed with azo form.

6. For the compounds **21**, **22** and **24** the coordination mode were determined by means of the IR spectra making the $\Delta\nu$ difference between the ν_{as} and ν_s of carboxylate groups of the polymer and those of the ionic compounds. In all these complexes the carboxylate anions interact directly with the metallic ion of the complex cation $[M(cyclam)]^{2+}$ (M = Ni^{2+}, Cu^{2+}). The polymers **21, 22** and **24** adopt a monodentate coordiation mode.

7. In the case of coordination polymers **26** and **27** the fumarate anions do not interact with metallic ion of the complex cation $[M(cyclam)]^{2+}$ (M = Ni^{2+}, Cu^{2+}). Instead, the water molecules preferentially coordinate to Cu^{2+} or Ni^{2+} in the DMF/H_2O cosolvents. The coordination behaviors of carboxylate groups of fumarate are highly dependent on the presence of additional hydrogen bonding interactions that reinforce the formation of the coordination polymers. These coordination polymers could be a good model systems for understanding of the nature of molecular interaction between $[M(cyclam)]^{2+}$ and carboxylate groups as well as the importance of the presence of hydrogen bonding in forming coordination polymers.

8. Coordination polymer **30** has a 3D network. Among the six nitrogen atoms of the macrocycle, only four are coordinated at metal atom, giving an ecuatorial plane belonging to a very distorted octahedron with axial positions occupyed by oxigen atoms from two different organic anions. We can notice accented asymmetry of the Cu-O bond length from axial positions in the case of both idependente octahedron fragments: Cu(1)–O(2) 2.304(3) Å / Cu(1)–O(12) 3.489(3) Å, and, Cu(2)–O(5) 2.300(3) Å / Cu(2)–O(9) 3.046(4) Å, respectively.

9. Have been performed investigations for the determination of the nature of coordination of the metallic center from complex cations $[M(cyclam)]^{2+}$ (M = Ni^{2+}, Zn^{2+}) by carmoisine using the conventional DFT with B3LYP exchange-correlation functional and the density functional-based tight binding (DFTB) methods. For a detailed understanding of the nature of the metal coordination, the *model system* built by two mesylate groups and $[M(cyclam)]^{2+}$ were considered. In the case of Ni^{2+} coordination complex singlet and triplet geometries are favored, in agreement with electronic configuration, $3d^8 4s^0$. For the Zn^{2+} complex, from energetically point of view, only singlet states is favored, according with electronic configuration $3d^{10} 4s^0$, the triplet configuration being forbidden.

10. For the compound **13** the BET area is 683 m^2/g, for **14** is 536 m^2/g, for **10** is 319 m^2/g and for **9** is 252 m^2/g. The others prepared polymers don't present permanent porosity. These areas of the BET surfaces are similarly to those of 560 m^2/g exhibited by {[Ni(tame)(4,4′-

bis(sulfoetinil)bifenil]} [(tame= tris(amino methyl)ethane], the single coordinating polymer reported in the literature data, as with those of some aza macrocycles coordination polymers (for example 817 m^2/g for [Ni(L_2)(BPyDC)] şi 691 m^2/g for [Ni($L3)_3$ ($BPDC)_3$]). The BET area surfaces of carboxylate coordination polymers are much smaller, for example a 39 m^2/g for compound **21** and only a 9 m^2/g for compound **24**.

11. Humidity sensor properties of the prepared polymers were studied. From all studied polymers only coordination polymer **5** exhibited such properties.

VI. SELECTIVE REFERENCES

1. Y. Kinoshita, I. Matsubara, T. Hibuchi, Y. Saito, *Bull. Chem. Soc. Jpn*., **1959**, *32*, 1221.
2. B. F. Hoskins, R. Robson, *J. Am. Chem. Soc.,* **1989**, *111*, 5962.
3. M. Kondo, T. Yoshitomi, K. Seki, H. Matsuzaka, S. Kitagawa, *Angew. Chem. Int. Ed*., **1997**, *36*, 1725.

4 S. L. James, *Chem. Soc. Rev*., **2003**, *32*, 276.

8. O. M. Yaghi, M. O'Keeffe, N. W. Ockwig, H. K. Chae, M. Eddaoudi, J. Kim, *Nature*, **2003**, *423*, 705.
10. E. Coronado, J. R. Galan-Maskaros, C. J. Gomez-Garcea, V. Laukhin, *Nature*, **2000**, *408*, 447.
11. O. Kahn, *Accounts Chem. Res.,* **2000***, 33,* 645.
12. B. Moulton, J. Lu, R. Hajndl S. Hariharan, M.J. Zaworotko, *Angew. Chem. Int. Ed*., **2002**, *41*, 2821.
13. D. B. Mitzi, C. A. Field, W. T. A. Harrison, A. M. Guley, *Nature,* **1994***, 369*, 467.
14. W. Lin, L. Ma, Z. Wang, *J. Am. Chem. Soc.*, **1999***, 121*, 11249.
15. N. L. Rosi, M. Eddaoudi, D. T. Vodak, J. Eckert, M. O'Keeffe, O. M. Yaghi*Science*, **2003**, *300*, 1127.
16. R. Kitaura, K. Seki, G. Akiyama, S. Kitagava, *Angew. Chem. Int. Ed*., **2003**, *42*, 428.
17. K. S. Min, M. P. Suh, *J. Am. Chem. Soc*., **2000**, *122*, 6834.
18. O. M. Yaghi, H. Li, *J. Am. Chem. Soc.,* **1996**, *118,* 295.
19. J. Seo, D. –M. Whang, H. –Y. Lee, *Nature*, **2000**, *404*, 982.
20. T. Sawaki, Y. Aoyama, *J. Am. Chem. Soc*., **1999**, *121*, 4793.
21. M. Albrecht, M. Lutz, A. L. Spek, G. van Koten, *Nature*, **2000**, *406*, 970.
22. J. A. Real, E. Andrés, M. Muños, M. Julve, T. Granier, A. Bousseksou, F. Varret , *Science*, **1995**, *268*, 265.
23. L. G. Beauvais, M. P. Shores, J. R. Long, *J. Am. Chem. Soc., **2000**, 122,* 2763.
24. O. R. Evans, W. Lin, *Chem Mater*., **2001**, *13*, 2075.
25. B. H. Hong, S. C. Bae, C. W. Lee, S. Jeong, K.S. Kim, *Science*, **2001**, *294*, 348
26. P. H. Dinolfo, J. T. Hupp, *Chem. Mater*., **2001**, *13*, 3113.
27. L. Pan, K. M. Adams, H. E Hernandez., X. Wang, C. Zheng, Y. Hattori, K. *J.* Kaneko, *Am. Chem. Soc., 2003, 125,* 3062.
28. J. L. C. Rowsell, A. R. Millward, K. S. Park, O. M. Yagi, *J. Am. Chem. Soc.,* **2004***, 126,* 5666.
29. G. Férey, M. Latroche, C. Serre, F. Millange, T.Loiseau, A. Percheron-Guégan. *Chem. Commun*., **2003**, 2976.
30. L. Pan, M. B. Sander, X. Y. Li, J. Huang, M. Smith, E. Bittner, B. Bockrath, J. K Johnson, *J. Am. Chem. Soc.,* **2004***, 126,* 1308.
31. A. M. Seayad, D. M. Antonelli, Adv. Mater., **2004**, *16*, 765.

44. S. Horike, R. Matsuda, D. Tanaka, M. Mizuno, K. Endo, S. Kitagawa, *J. Am. Chem. Soc*., **2006**, *128*, 4222.
48. M. P. Suh, H. R. Moon, *Advanced Inorg. Chem*., **2007**, *59*, 39.
49. M. P. Suh, Y. E. Cheon, E. Y. Lee, *Coord. Chem. Rev.,* **2008**, *252*, 1007.
54. H. J. Choi, T. S. Lee, M. P. Suh, *Angew. Chem. Int. Ed*., **1999**, *38*, 1405.
99. H. Kim, M. P. Suh, *Inorg. Chem*., **2005**, *44*, 810.
135. C. H. Chen, C. Ken, J. Cai, C.-Z. Liao, X.-L. Feng, X.-M. Chen, S. W. Ng, *Inorg. Chem*., **2002**, *41*, 4967.
136. C. H. Can, C.-H. Chen, J.-S. Zhou, *Chin. J. Inorg. Chem.*, **2003**, *19*, 81.
137. P. V. Bernhardt, T. E. Dyahningtyas, S. C. Han, J. M. Harrowfield, I. C. Kim, Y. Kim, G. A. Koutsantonis, E. Rukmini, P. Thurey, *Polyhedron*, **2004**, *23*, 869.
138. J. Cai, C.-H. Chen, C.-Z. Liao, J.-H. Yao, X.-P. Hu, X.-M. Chen, *J. Chem Soc*., *Dalton Trans*., **2004**, 1137.
139. X. Ribas, D. Maspoch, K. Wurst, J. Veciana, C. Rovira, *Inorg. Chem*., **2006**, *45*, 5383.
140. A. J. Shunbnell, E. J. Kosnic, Ph. Squattrito, *Inorg.Chim. Acta,* **1994**, *216*, 101.
141. S. E. Forest, R. L. Kuczkowski, *J. Am. Chem. Soc.,* **1996**, *118*, 217; W. H. Ojala, E. A. Sudbeck, L. K. Lu, T. I. Richardson, R. E. Lovrien, *Acta Crystallogr., C50*, **1994**, 1615; C. F. J. Faul, M. Antonietti, W. Massa, *Acta Crystallogr., E60*, **2004**, 1769.
142. W. H. Ojala, L. K. Lu, K. E. Albers, W. B. Gleason, T. I. Richardson, R. E. Lovrien, E. A. Sudbeck, *Acta Crystallogr. B50*, **1994**, 684.
143. L. Kisong, H. Wang, J. Vhen, Zh. Wabg, J. Sun, D. Zhao, Y. Yan, *Microporous and Mesoporous Materials,* **2003**, *58*, 105.
144. K. Wojciechowski, S. Jerzy, *Dyes and Pigments* **2000**, *44*, 137.
145. G. Socrates, Infrared Characteristic Group Frequencies, John Wiley and Sons, New York, **1980**.
146. N. Peica, Dissertation, Vibrational spectroscopy and density functional theory calculations on biological molecules, Würtzburg, **2006**.
147. a/ M. R. Almeida, R. Stephani, H. F. Dos Santos, L. F. C. De Oliveira, *J. Phys. Chem.*A **2010**, *114*, 526.
b/ N. Biswas, S. Umpatathy, *J. Phys. Chem.* A **1997**, *101*, 5555.
c/ H. F. Dos Santos, L. F. C. De Oliveira, S. O. Dantas, P. S. Santos, W. B. De Almeida, *Int. J. Quant. Chem*., **2000**, *80*, 1076.
148. J. Dinda, U. Ray, G. Mostafa, T. H. Lu, A. Usman, I. A. Razak, S. Chantrapromma, H. K. Fun, C. Sinha, *Polyhedron,* **2003**, *22*, 247.
149. U. S. Ray, G. Mostafa, T. H. Lu, C. Lu, C. Sinha, *Crystal Engineering* **2002**, *5*, 95.
150. P. Byabartta, S. Jasimuddin, B. K. Ghosh, C. Sinha, A. M. Z. Slawin, J. D. Woollins, *New J. Chem*., **2002,** *26*, 1415.
151. T. H. Lu, T. K. Misra, P. C. Lin, F. L. Liao, C. S. Chung, *Polyhedron,* **2003**, *22*, 535.

152. F. R. Allen, O. Kennard, D. G. Watson, L. Brammer, A. G. Orpen, R. J. Taylor, *J. Chem. Soc. Perkin Trans., 2,* **1987**, S1.
153. J. Dinda, K. Bag, C. Sinha, G. Mostafa, T. H. Lu, *Polyhedron,* **2003**, *22*, 1367.
174. N. Nakamoto, Infrared and Raman Spectra of Inorganic and Coordination Compounds, sixth ed., John Wiley &Sons Publishers, New Jersey, **2009**.
184. J. Y. Lee, J. Jagiello, *J. Solid State Chem.*, **2005**, *178*, 2527.
208. S. A. Moiz, S. Kh. Karimov, N. D. Gohar, *Euroasian Chemico-Technological Journal*, **2004**, *6*, 179.
209. S. A. Moiz, M. M. Ahmed, S. Kh. Karimov, *Jap. J. Appl. Phys.*, **2005**, *44*, 1199.
210. Zubair, M. H. Sayyad, M. Saleem, S. Kh. Karimov, M. Shah, *Physica E: Low-dimensional System and Nanostructures*, **2008**, *41*, 18.
211. Shah, M. H. Sayyad, S. Kh. Karimov, *World Academy of Science, Engineering. and Technology*, **2008**, *43*, 392.
212. K.Y. Law, *Chem. Rev.*, **1993**, *93,* 449.
213. R. Taguchi, T. Cobayashi, J. Muta, *J. Mater, Sci. Lett.*, **1994**, *13*, 1320.
221. T. M. Hunter, I. W. McNae, X. Liang, J. Bella, S. Parsons, M. D. Walkinshaw, P. J. Sadler, *Proc. Nat. Acad. Sci. USA*, **2005**, *102*, 2288.
222. L. F. Lindoy, M. S. Mahinay, B. W. Skelton, A. H. White, *J. Coord. Chem.*, **2003**, *56*, 1203.
223. K. Mochizuki, T. Kondo, *Inorg.Chem.*, **1995**, *34*, 6241.
225. J. Emsley, *Die Elemente*, Walter de Gruyter, Berlin, **1994**.
227. S.-L. Ma, Y. Ma, S. Ren, S.-P. Yan, D.-Z. Liao, *Struct. Chem.*, **2008**, *19*, 329.

Appendix 1

TEM images of some coordination polymer crystals synthesized. TEM scale is given in the brackets.

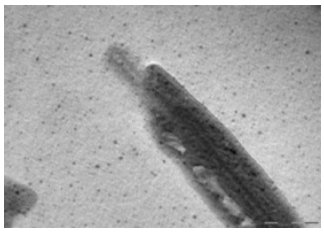

PC 5; (**20nm**)

$[\{Cu(ciclam)\}_3(trt)_2\cdot 6H_2O]_n$

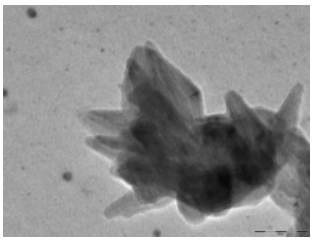

PC 6; (**50nm**)

$[\{Ni(ciclam)\}_3(trt)_2\cdot 43H_2O]_n$

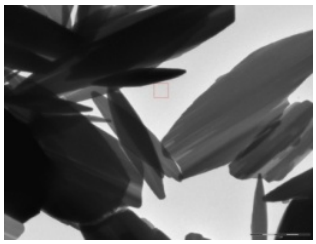

PC 10; (**2μm**)

$[Ni(ciclam)(crmz)]_n$

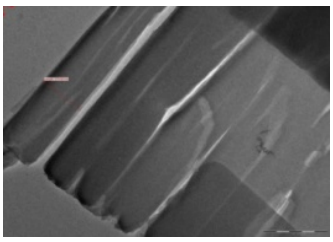

PC 12; (**500nm**)

$[\{Cu(ciclam)\}_3(amrt)_2\cdot 13H_2O]_n$

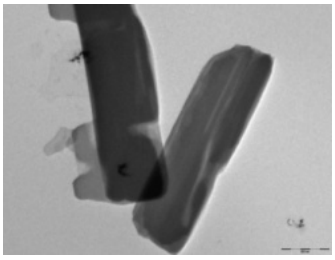

PC 13; (**500nm**)

$[\{Ni(ciclam)\}_3(amrt)_2\cdot 4H_2O]_n$

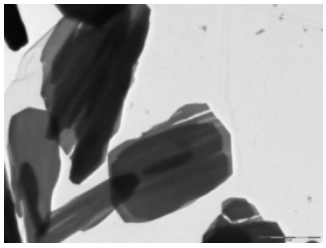

PC 14; (**500nm**)

$[\{Zn(ciclam)\}_3(amrt)_2\cdot 14H_2O]_n$

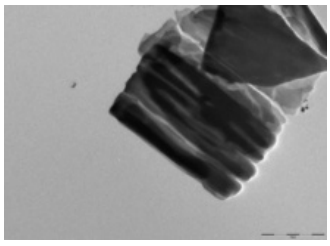

PC 12; (**1μm**)

$[\{Cu(ciclam)\}_3(amrt)_2\cdot 13H_2O]_n$

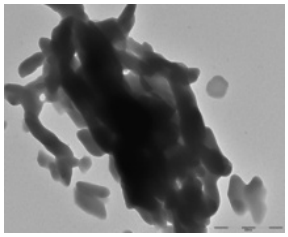

PC 16; (**500nm**)

$[Ni(ciclam)(ssyw)\cdot 0.5H_2O]_n$

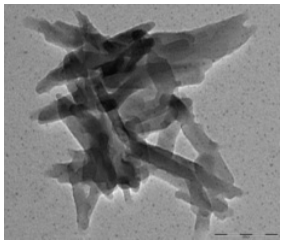

PC 18; (**100nm**)

$[Cu(ciclam)(rcg)]_n$

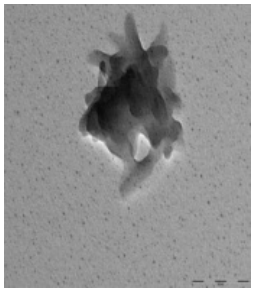

PC 19; (**100nm**)

$[Zn(ciclam)(rcg)]_n$

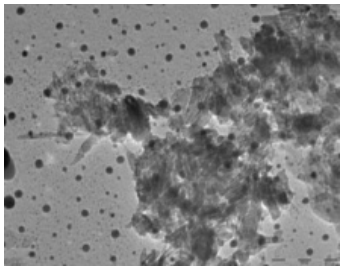

PC 27; (**100nm**)

$[\{Ni(ciclam)(H_2O)_2\}(fum)\cdot 4H_2O]_n$

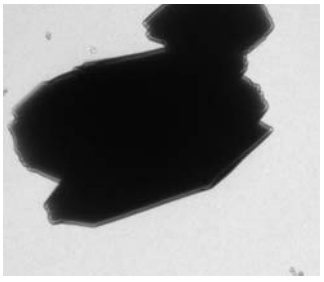

PC 26; (**500nm**)

$[\{Cu(ciclam)(H_2O)_2\}(fum)\cdot 4H_2O]_n$

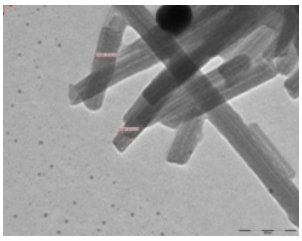

PC 30; (**100nm**

$[\{Cu(hatco)\}_2(tcm)\cdot 11H_2O]_n$

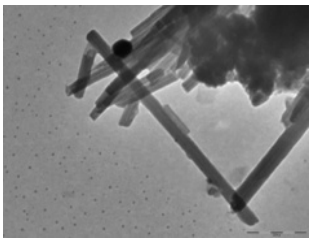

PC 30; (**200nm**)

$[\{Cu(hatco)\}_2(tcm)\cdot 11H_2O]_n$

1. **SCIENTIFIC PUBLICATIONS**

2.

3. **M. Vlassa**, G. Borodi, A. Biris, G. Blanita, M. Vlassa, C. Silvestru, Characterization by vibrational spectroscopy of coordination polymers obtained from Cu^{II}, Ni^{II} and Zn^{II} cyclam perchlorate and amaranth, *Rev. Roum. Chim.,* ***2011****, acceptată, în curs de tipărire.*
4. **M. Vlassa**, G. Borodi, G. Blănița, I Cojocaru, M. Vlassa, C. Silvestru, Synthesis and characterization of coordination polymers prepared from Cu^{II} and Ni^{II} cyclam perchlorate and carmoisine *Cent. Eur. J. Chem*., **2011** *9(2),* 224-231 DOI: 10.2478/s11532-010-0141-9.

2 SCIENTIFIC COMMUNICATIONS

1 M. Vlassa, C. Silvestru G. Borodi, M. Vlassa, **Characterization by thermogravimetric and crystallographic methods of $\{[Cu^{II}(cyclam)(H_2O)_2](fumarate)(H_2O)_4]\}_n$ and $\{[Ni^{II}(cyclam)(H_2O)_2](fumarate)(H_2O)_4]\}_n$ Coordination Polymers** *17 ISSS News and Beauty in Separation Sciences, International Symposium on Separation Science, CEGSS*, *September 5th-9th, **2011**, Cluj-Napoca,* Book of Abstracts ISBN 978-973-133-981-8 p.135, http://www.17isscluj2011.org

2 M. Vlassa, G. Borodi, A. Biriş, A. Bende , G. Blănița, D. Lupu, M. Vlassa, C. Silvestru. **Synthesis and Characterization of Coordination Polymers Obtained from Cu^{II} and Ni^{II} Cyclam Perchlorate and Carmoisine**, *ICOSECS 7, Chemystry-Beauty and Application, International Conference of the Chemical Societies of the South-Eastern European Countries, September 15th-17th, **2010**, Bucharest,* Book of Abstracts ISBN 978-973-748-512-0 p.204 ,http://www.icosecs7.upb.ro(Comunicare orală)